Causality Study of Pressure Effects on Hall Thruster Telemetry

IEPC-2025-580

Presented at the 39th International Electric Propulsion Conference Imperial College London • London, United Kingdom 14-19 September 2025

Seth J. Thompson¹, Colorado State University, Fort Collins, CO 80523, USA

Kentaro Hara², Stanford University, Stanford, California 94305, USA

Janice Cabrera³, Mitchell Walker⁴, Georgia Institute of Technology, Atlanta, GA, 30332, USA

and John D. Williams⁵ Colorado State University, Fort Collins, CO 80523, USA

Understanding the effect of the vacuum test facilities on the dynamics of Hall thrusters is a crucial step towards advancing time-resolved models used for predictive ground-to-space simulations. We investigate how chamber pressure reshapes the information flow among common telemetry signals. Using extended convergent cross mapping (eCCM), we analyzed time-synchronized measurements of discharge voltage, cathode current, and cathode-toground voltage from an H9 thruster operating on krypton at 300V and 15A in Georgia Tech's VTF-2 at a baseline pressure of 6.8 μTorr, and at two elevated pressures (2× and 3× baseline). To select embedding parameters, we parametrically swept time delay τ and embedding dimension m to maximize cross-mapping skill (Pearson correlation between real and reconstructed signals) before applying time shifts to inform causal strength and directionality. At baseline pressure, discharge voltage and cathode-to-ground voltage appear to be causally influenced by cathode current. Links involving reconstruction of cathode-to-ground voltage often peak at positive lags, consistent with generalized synchrony rather than direct causation, further complicating direct causal analysis. As pressure increases, cross-mapping skill declines across pairs, with the strongest degradation in reconstructions by cathode-to-ground voltage, suggesting that pressure-enabled effects are likely to impact the dynamics of cathodeto-ground voltage. Throughout all pressures, discharge voltage remains the most informative predictor of the other telemetry, making it a valuable probe for dynamic modeling. These results clarify which measurements carry dynamically relevant signal content and show how elevated facility pressure erodes it—evidence that is useful for ground-to-space extrapolation and for selecting telemetry in time-resolved models.

⁵ Professor, Mechanical Engineering, Colorado State University, john.d.williams@colostate.edu



¹ Research Associate, Mechanical Engineering, Colorado State University, seth.thompson9@gmail.com

² Assistant Professor, Aeronautics and Astronautics, Stanford University, kenhara@stanford.edu.

³ PhD Candidate, Aerospace Engineering, Georgia Institute of Technology, Janice.d.cabrera@gatech.edu

⁴ Professor, Aerospace Engineering, Georgia Institute of Technology, mitchell.walker@ae.gatech.edu

I.Introduction

Predictive Hall thruster modeling necessitates the identification of key model elements required to describe observable dynamics. Both Hall thruster and hollow cathode discharges exhibit non-linear dynamic behavior as a result of the underlying physics of their respective plasma discharges. Capturing these independent behaviors provides useful information in their own right; however, in typical thruster operation, these two dynamical systems are forced to interact through one DC power supply. Further complicating the picture is the addition of a third actor, present in all ground testing that is not present in-flight conditions – ground test facilities, i.e., vacuum chambers. Understanding how these dynamics are affected by the environment in which they are tested will help reduce uncertainty in ground-to-space predictions.

To better capture the critical elements required to understand thruster dynamics, we propose using the extended cross convergent mapping framework [1] developed as an extension of dynamic causality methods first introduced by Sugihara et al. [2] and previously applied to dynamic signals in Hall thruster simulation [3] and experimental measurements [4], to evaluate how dynamics in commonly measured thruster telemetry (voltage and current measurements) are impacted by increasing facility pressure. We apply the dynamic analysis to H9 discharge voltage, cathode current, and cathode-to-ground voltage as the thruster is operated at three operational pressures in Vacuum Test Facility 2 (VTF-2) at the Georgia Institute of Technology High Power Electric Propulsion Laboratory (HiPEPL). We discuss key considerations and limitations of the analysis and results as well as provide guidance on application to further facility tests.

II. Cross-convergent mapping (CCM) for causality analysis

To understand the relationship between dynamic signals of Hall thruster telemetry, we employ extended cross-convergent mapping (e-CCM). The original work of cross-convergent mapping (CCM) was first brought to the floor by Sugihara in 2012 to distinguish causality from correlation in dynamic systems. The CCM method aimed to address the shortcomings of using Granger-causality on dynamic systems where separability of system variables could not necessarily be achieved [2]. The premise of CCM relies on nonlinear state-space reconstruction that leverages Taken's theorem [5] to assert that in a deterministic dynamic system, if one variable x is causal on another y, then the dynamic history of x will be present in the dynamics of y. The process then follows to attempt to reconstruct the dynamic signals of the timeseries x(t) from a delayed embedding (sometimes called a shadow manifold) of the timeseries y(t). If this reconstruction can be performed with increasing accuracy, as measured by the Pearson correlation coefficient, ρ , between the reconstructed and real time series, when more data are included in the analysis, then it can be understood that x to y is causal.

Then, in 2015, Ye et al. extended this framework to address further difficulties of interpreting CCM results in systems with generalized synchrony or strong unidirectional forcing that could lead to ambiguous results from standard CCM [1]. By shifting one signal with a time shift (l) relative to another prior to reconstruction of any signals, peaks in reconstruction quality can be observed when signals are reconstructing past or future values of the other, indicating time delays between causal variables and distinguishing generally synchrony from bidirectional coupling. This improved context of the flow of information is useful for application to Hall thrusters, which can be dominated by a large global oscillation, such as the breathing mode, over which many other dynamic relationships may take place. If one signal can be used to capture large oscillations experienced by the entire system, this does not guarantee causal relationships to other variables responding to the same global oscillations.

For the sake of brevity, we exclude the details of the eCCM algorithmic process and direct the readers to any of the works of Huerta for detailed descriptions of the algorithm [3], [4], [6]. We do, however, want to outline the basic flow of the process. Time-resolved signals are collected synchronously for all variables of interest (thruster voltage and current in our case). The signals are split into test-train segments so that evaluation of the reconstructed signal can be performed on segments that do not directly overlap with training data. A nonlinear state-space reconstruction method is then used to reconstruct the time series of one signal from the other. This requires that the signal, y, used for reconstructing the other signal, e.g., x, must be used to generate a shadow manifold with time-delay embedding $M_y = [y(t), y(t-\tau), ..., y(t-m\tau)]$. Selection of the appropriate time delay (τ) and embedding dimension (m) is



required, and more details on the selection of these parameters are discussed in Section B. At each time step, we take the time-delay embedding test data manifold, i.e., $M_{y,test}(t=t_0) = [y_{test}(t=t_0), y_{test}(t=t_0-\tau), ..., y_{test}(t=t_0-\tau), ..., y_{test}(t=t_0-\tau)]$, and the train data manifold, i.e., $M_{y,train}(t=t_1) = [y_{train}(t=t_1), y_{train}(t=t_1-\tau), ..., y_{train}(t=t_1-(m-1)\tau)]$. Then, we find a finite number of t_1 values of the train data manifold that result in the Euclidean distance between $M_{y,test}(t_0)$ and $M_{y,train}(t_1)$ to be small, which can be called the near-neighbors. Using the t_1 values that are found, a shadow manifold of x, i.e., $\widehat{M_x}(t)$, is constructed using the $M_{x,train}(t_1)$ values. From the constructed manifold $\widehat{M_x}(t) = [x_{est}(t), x_{est}(t-\tau), ..., x_{est}(t-(m-1)\tau)]$, $\widehat{x}(t)$ can be estimated by taking an average of m values of $x_{est}(t)$. The Pearson correlation coefficient ρ is used to evaluate the reconstructed signal $\widehat{x}(t)$ and the test signal $x_{test}(t)$. The length of data L used for the reconstruction is gradually increased to demonstrate the convergence of the mapping [2].

This extended cross-convergent mapping (eCCM) framework has been applied by Huerta et al. to Hall thruster simulations [3] and experimental Hall thruster data [4]. The application of eCCM to the experimental measurements was employed to evaluate how dynamic current information propagated to and from a Hall thruster operated in a unique enclosure that enables measurement of current to surfaces around the Hall thruster while allowing neutral density to escape to the surrounding vacuum pumps. Furthermore, Huerta employed other causality analysis tools, such as reservoir computing-based causality (RCC) and transfer entropy (TE), in addition to eCCM, to compare their performance on these dynamic current data [6]. We first apply this analysis to logistic equations as an example, followed by a discussion of embedding parameter selection for the telemetry signals. We then employ eCCM to evaluate the H9 telemetry signals and discuss the results in the context of understanding changes in the dynamic relationships of circuit elements as the thruster is operated under different power levels and pressure conditions.

A. Example of General Synchrony

To demonstrate the technique and typical interpretation of the results, we apply eCCM to coupled logistic equations used in previous demonstrations [6]. In our example, we have selected two time-dependent variables, X and Y, that are driven by a third Z. In addition, we have included the ability to delay the response of X to Z with the delay parameter k.

$$Z(t+1) = Z(t)(A_z - A_z Z(t))$$

$$Y(t+1) = Y(t)(A_y - A_y Y(t) - B_{yz} Z(t))$$

$$X(t+1) = X(t)(A_x - A_x Y(t) - B_{xz} Z(t-k))$$
(1)

For the following eCCM results presented in Figure 1-Figure 3, all coefficients are kept the same, $A_z = 3.8$, $A_y = 3.1$, $A_x = 3.1$, $B_{yz} = 0.9$, $B_{xz} = 0.5$, and the initial values of X(0), Y(0), Z(0) = 0.3, with the only difference in the tests being an adjustment to a delay parameter k. These values are chosen as a test to demonstrate how a strongly driven system, where Z causes X and Y, may then result in ambiguity of relationships between X and Y themselves, since they will likely both reconstruct well owing to the strong coupling with Z.

Embedding parameters used for reconstruction were selected from a parameter sweep of the embedding delay τ and embedding dimension m that resulted in the highest reconstruction coefficient for each reconstruction. This process is discussed in greater depth in Section B, but m was between 5-7 (depending on which signal was reconstructing what other signal), while $\tau=2$ for all reconstructions. The process is repeated for several segments of the time series to allow for the capture of variation depending on the dataset used. The solid lines in all figures represent the mean of the segments, while the shaded regions are one standard deviation from the mean. For all results, the cross-mapping skill is defined using the Pearson correlation coefficient ρ between a test and reconstructed signal.



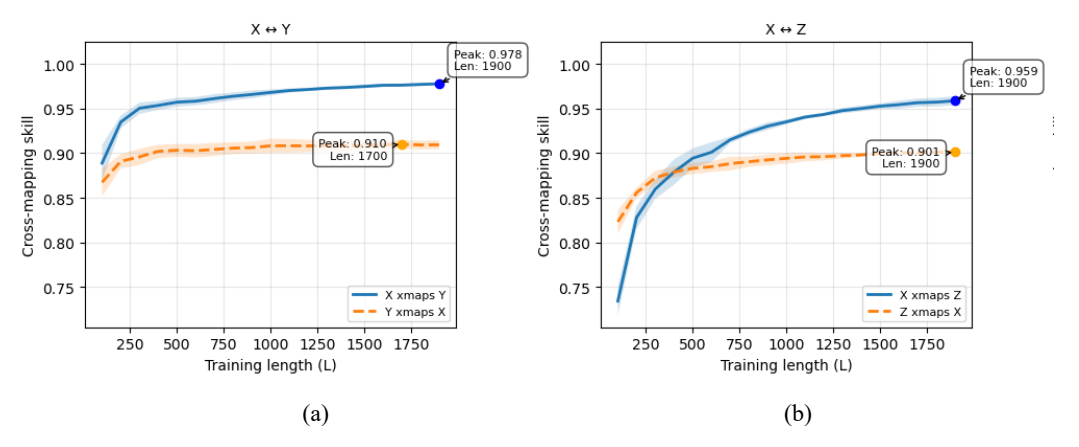


Figure 1: Cross-mapping skill of X and Y from equation 1 with increasing data length (L), with false links identified between X and Y owing to general synchronicity from the common forcing variable Z, with no applied time shift (l = 0) and k = 2.

Figure 2 shows the cross-mapping skills with increasing training data length. The nomenclature "X xmaps Y" refers to the case where the signal X is used to reconstruct a test segment of Y. In traditional cross-convergent mapping, an increasingly higher cross-mapping skill with increased signal length L indicates a causal link between the variables. However, as can be seen by the improved reconstructions between X and Y with increasing data length in shown in Figure 1(a), false links, convergence behavior of cross-mapped variables that are not causally related, can be established if both variables are strongly driven by some other variable that makes the variables generally synchronous. In this case, both the blue and orange curves show increases in cross-mapping skill with increased data length. Furthermore, signals with strong unidirectional coupling may indicate bi-directional causal relations, illustrated by cross-mapping of X and Z in Figure 1(b). Both X and Z display convergent behavior, with the blue and orange curves both showing higher cross-mapping skill with increasing data length, but Z cross-mapping X well is the result of how strongly X is coupled to Z, and not any causal influence of Z by X, as may be interpreted in traditional CCM. This is where time-shifting signals with respect to one another, as done in extended cross-convergent mapping, can provide more context.

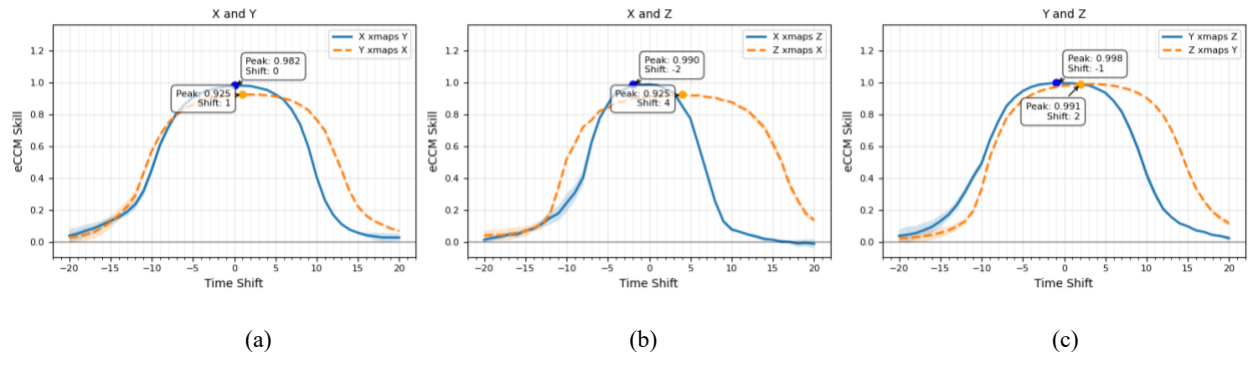


Figure 2: Extended cross-mapping results of equation (1) with the delay k = 0, with accurate identification of Z's causal effect on X and Y but ambiguous results of how X and Y relate to each other.

Extended cross-mapping of the signals in Figure 2 shows the reconstructions that are made after one signal is shifted either forward or backward with respect to the other signal it was attempting to reconstruct. If a reconstruction of a signal has a peak cross-mapping skill with a negative time shift, this indicates that the signal being cross-mapped is causal on the signal used to reconstruct it, with the magnitude of the negative shift indicative of roughly the delay between variables. In Figure 2(b), the peak of "X xmaps Z" is -2 steps, indicative of Z being causal on X as designated in equation (1). If the peak reconstruction value of the other signal is forward shifted, then this indicates the quality of



the reconstruction is the result of generalized synchrony of the system, in this case the variable doing the driving Z. Generalized synchrony is a case where the system dynamics are strongly dominated by a driving set of dynamics that cause other, potentially non-causally related variables, to reconstruct well due to a common mutual dynamic information of the system. Often, if the system is generally synchronous, there will be peaks in cross-mapping skill with a positive time shift due to the delay in propagation of the strong dynamics throughout the system to the variable being reconstructed. This is illustrated by "Z xmaps X" in Figure 2(b). In this case, Z drives X, but peak reconstruction occurs with a forward shift because X is responding to the dynamics of Z. The same relationship is also observed for Y and Z shown in Figure 2(c).

Systems with general synchrony and disparity in response lag between variables face an additional challenge, whereby two variables that are not causally related at all may appear to be a case of unidirectional forcing, as shown by "Y xmaps X" in Figure 3(a). In Figure 3, we show the eCCM results of equation (1) with the response of X delayed by setting k = 2, resulting in X responding slower than Y to the common driving variable Z. The peak in crossmapping skill "X xmap Y" being negative, while the reciprocal has a positive time shift, indicates a relationship similar to X and Z or Y and Z from Figure 2. However, by looking at the cross-mapping skills of the other variables, Figure 3(b) and Figure 3(c), we can see that both X and Y appear to be causally influenced by Z, with a longer response delay for X. From here, it can be deduced that Y acting causally on X is a false link owing to the higher cross-mapping skill and identification of response delays with the inclusion of Z. This example underscores the complexity of attempting to evaluate causality in systems with high degrees of generalized synchrony, especially in cases of differing response delays, and we must understand that incomplete evaluation of the system parameters may not conclusively determine causal links between a subset of system variables.

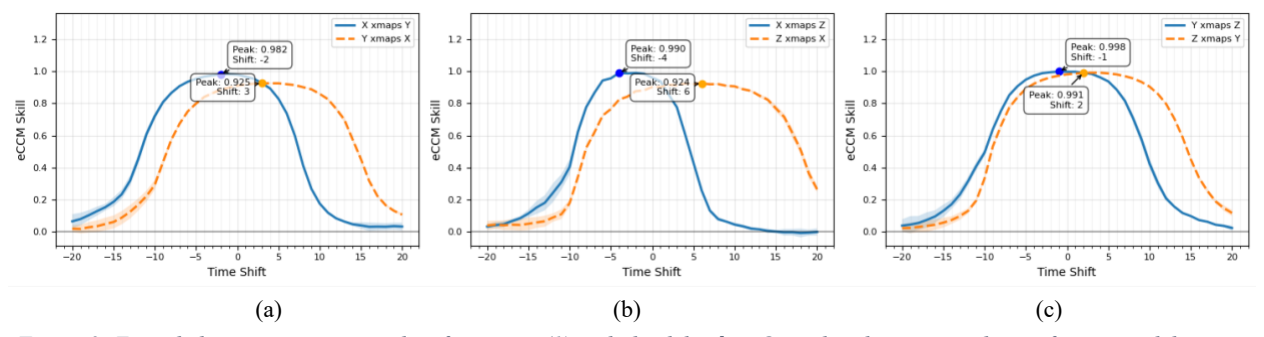


Figure 3: Extended cross-mapping results of equation (1) with the delay k = 2 used to demonstrate how information delays can complicate the interpretation of uncoupled variables X and Y.

B. Embedding parameter selection

Selecting time delay and embedding dimensions is required to generate a shadow manifold used to reconstruct a test signal in the cross-mapping process. Specifically, a time delay τ and embedding dimension m must be selected. Mathematically, the only requirement, as a result of Taken's Theorem [5], is that the embedding dimension be greater than twice the dimension of the underlying dynamical system m = 2d + 1, where d is the actual number of attractor dimensions of the underlying system. Hence, from a time series signal x(t), we consider a m-dimensional portrait:

$$[x(t), x(t-\tau), x(t-2\tau), x(t-m\tau)].$$

The time-delayed phase portrait was first introduced to the EP community by Greve et al. [7]. There is no requirement τ to generate a mathematically proper embedding; however, real-world applications demonstrate that both embedding dimensions and time delay have significant impacts on the quality of the reconstructions. Throughout the years, many heuristics for determining relevant time delay τ and embedding dimension m have been developed.

Cao's method, based on a modified form of identifying false-near neighbors, has been used in many applications with thruster-relevant signals [4], [6] for selecting m. However, this process requires the selection of a time delay, which historically has had a large number of heuristics proposed for a given application [8]. Recently, work by Martin



et al. [9] has demonstrated a robust framework that leverages the mutual information of transformed coordinates (MITC) to select a good estimate for τ . This framework requires the selection of the number of dimensions to include in the analysis. This technique, along with Cao's method, was explored in the initial analysis of the H9 thruster telemetry signals. However, we observed cases where significant improvements were seen when using different embedding parameters for a given set of signals being analyzed. This was likely due to selecting too few dimensions for the MITC analysis and too low a convergence threshold for the Cao method. Further evaluation of understanding how best to leverage MITC and the Cao methods to select embedding dimensions is left to future work. For reconstructions of the H9 telemetry signals, the embedding parameters were selected from a parametric sweep of τ and m, and the pair of embedding dimensions and time delay that resulted in the highest reconstruction quality for a given pair of signals. These sweeps are repeated for reconstruction in the reciprocal direction as well. Therefore, every pair of signals reconstructing one another used the embedding dimension m and the embedding time delay τ that produced the best reconstruction with no time shift applied.

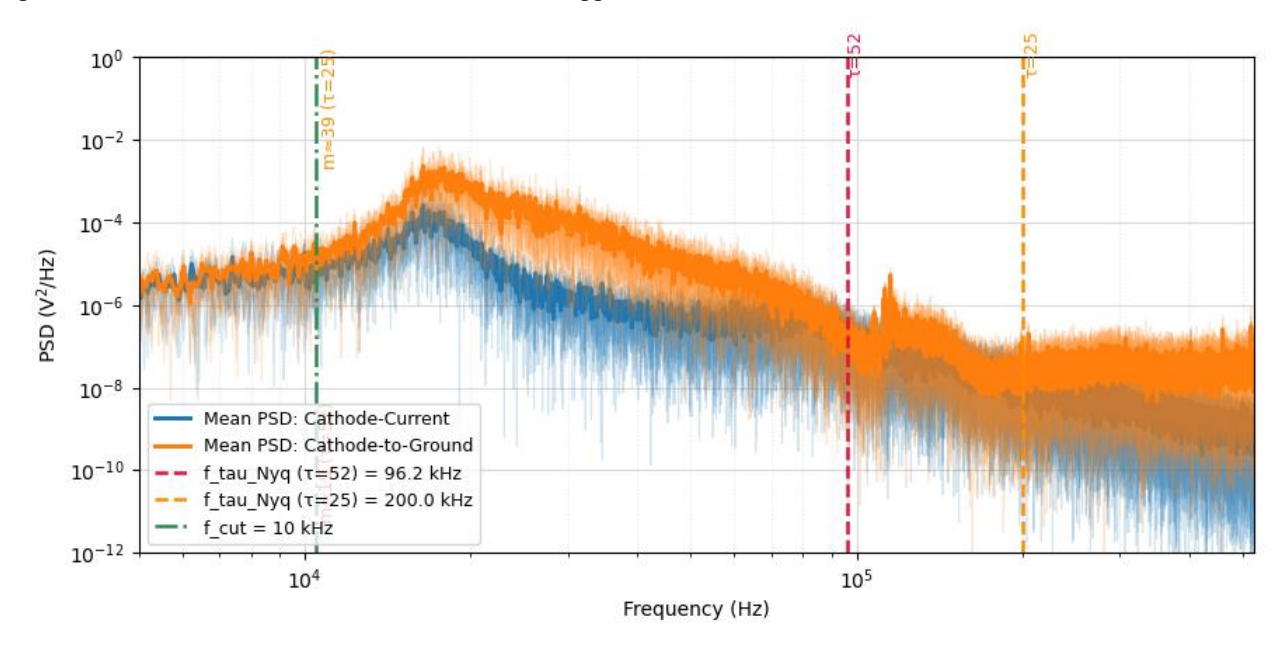


Figure 4: Power spectral density plot of the cathode current and cathode-to-ground voltage operated at 300V and 15A at the baseline pressure of 6.8 µTorr with the PSD of the entire waveform and averaged PSD values of 8 segments of each signal.

Determining a relevant range of τ and m values for which to scan across can be informed by knowledge of the power spectra of the signal and limitations of the devices used to measure the signals. In our case, the smallest values of τ can be thought of as the shortest time period that the embedding will capture changes. At the same time, the $m\tau$ will limit the longest timescale (smallest frequency) captured by a given embedding vector in the manifold. In our case, there is a limit to the believable highest frequency range that can be measured with the probes used, due to bandwidth limitations and noise. We also know from the PSD plot of the signals being evaluated that a $m\tau$ product that captures a frequency lower than the breathing mode would contain a large portion of the signal strength. Figure 4 shows a PSD plot with the minimum frequencies of two different time lag selections, as well as the number of dimensions m that would be required to achieve a frequency below 10 kHz, which is inclusive of much of the breathing mode width. In our data sets, $\tau = 1$ it corresponds to the temporal resolution of the data, i.e., 5 MHz (0.2 μ s).

A parametric sweep to evaluate how time delay (τ) and embedding dimension (m) affect the reconstruction skill of cathode current from cathode-to-ground voltage was performed across a wide range of values, as shown in Figure 5. Annotations showing representative time delays and embedding dimensions from Figure 4 are shown, as well as



the maximum reconstruction quality. Although there is more information in the cathode-to-ground signal at frequencies above 200 kHz, as τ shown in both figures, it did not add a significant amount of reconstruction skill to select lower and lower time delays for the purposes of reconstructing cathode current. It was observed that maximum reconstructions followed a constant τm product, as shown in Figure 5. This can be thought of as the minimum window length required to capture the dynamic frequency range discussed in Figure 4. This process was repeated for each pair of signals and in each direction of cross-mapping, for example, X to Y and from Y to X, with all signal pairs presented in the results. These parametric sweeps of τ and m are conducted with no time shift applied between the two signals.

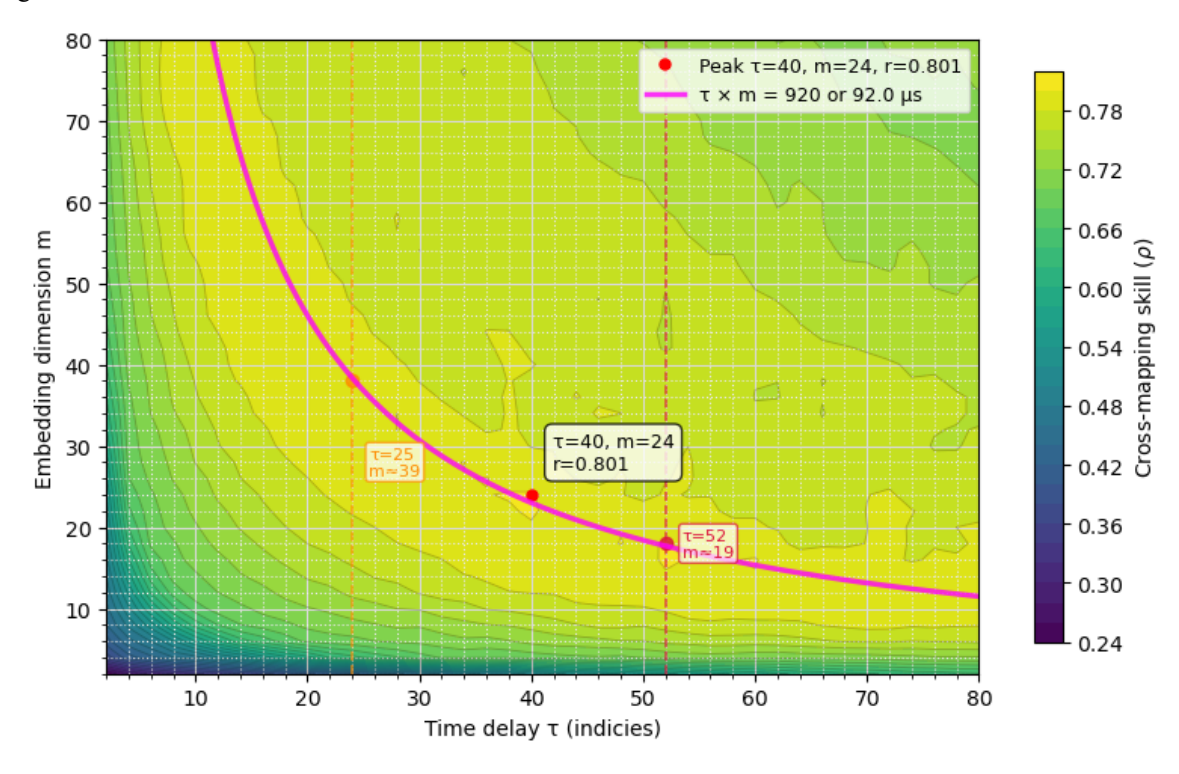


Figure 5: Parametric sweep of embedding parameters of time delay (τ) and dimension (m) for cathode-to-ground with constant τm product of 92 μs shown.

C. Experimental Setup

We applied the extended cross-convergent mapping analysis to Hall thruster telemetry data collected in a previous facility pressure effect test on thruster impedance presented in [10]. This test was conducted with an H9 magnetically shielded Hall thruster developed by the University of Michigan, Air Force Research Laboratory, and Jet Propulsion Laboratory [11] and operated on krypton in VTF-2 at HiPEPL. The lowest operational pressure for the thruster at the 4.5 kW operating condition was 6.8×10^{-6} Torr. Telemetry data was captured with a Teledyne Lecroy Digital Oscilloscope HDO6104, with Powertek DP-25 differential voltage probes (bandwidth of 25MHz) for both discharge and cathode-to-ground voltage measurements. Cathode current was measured with a Teledyne LeCroy CP150 current clamp (bandwidth of 5 MHz). Data from the oscilloscope was collected at 10 MHz. The thruster was operated with an RC filter to protect the power supply from large oscillations, with a resistance of 0.533 Ω and a capacitance of 100 μ F. The thruster was operated with the thruster body tied to the chamber-ground.



III. Results

We applied the extended cross-convergent mapping analysis to voltage and current signals for the H9 tested at the lowest achievable operating pressure (baseline), as well as twice (2x), and three times (3x) this pressure. The thruster was operated for several hours at the baseline pressure to reach a steady state operating mode. Slight shifts were observed in the dynamics throughout this period, and although these changes were not quantitatively analyzed to determine whether a dynamic steady-state was achieved, as discussed in work by Greve et al. [12], they were observed to exhibit more consistent voltage and current peak-to-peak and root mean squared values after operating for ~3 hours.

A. H9 - 4.5kW Baseline Pressure

The three thruster signals – discharge voltage, cathode current, and cathode-to-ground voltage were used to reconstruct each of the other signals collected synchronously. The reconstructions were compared to test signals from a 50/50 test-train split applied to windowed segments of the oscilloscope waveform that was collected. The windows were selected such that a test train split contained 51,200 data points, which contained ~ 70 breathing mode oscillations across the roughly 5 milliseconds. The average values for cross-mapping skill of all segments are the solid lines in Figure 6 through Figure 8 and while the shaded region represents one standard deviation from the mean, as discussed in Section II. B. The embedding dimension (m) and delay (τ) that reconstructed the signal most accurately in a parameter sweep with no time shift applied were used as the embedding parameters for all reconstructions at all time shifts.

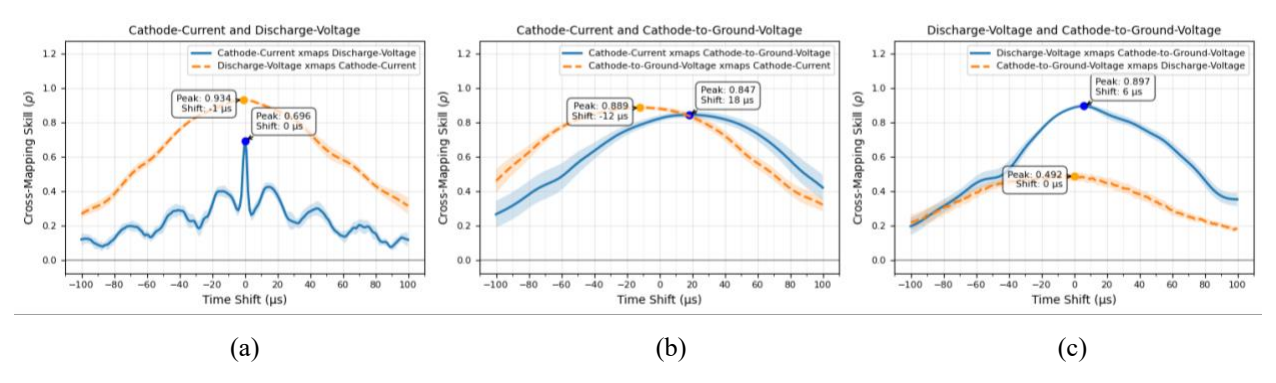


Figure 6: Cross-mapping skill of Hall thruster telemetry of the H9 thruster operating at 300V 15A at 6.8×10-6 Torr

The cross-mapping results of the telemetry for the H9 operated at 4.5 kW at a pressure of 6.8 μTorr are shown in Figure 6. Starting from Figure 6(a), we can see that the discharge voltage can reconstruct cathode current quite well and achieves a peak Pearson coefficient $\rho = 0.934$ at a time shift of -1 µs, indicating that discharge voltage is causally influenced by cathode current. However, the reciprocal reconstruction of the discharge voltage by cathode current is significantly lower $\rho = 0.696$ at a time shift of 0 µs. This is likely the result of the general synchrony of the system. Figure 6(b) shows a good example of unidirectional forcing described in the example eCCM test in Section II.A. Here, the cathode-to-ground voltage cross-maps cathode current with greater accuracy than in the other direction, along with a peak at a negative time shift of -12 µs. The positive time shift peak of cathode current cross-mapping cathode-to ground voltage would then indicate generalized synchrony with unidirectional forcing, shown clearly in our coupled logistic examples and by Ye et al. [1]. This negative and positive shift of peak cross-mapping skill implies that cathodeto-ground voltage is sufficiently influenced by cathode current, such that despite cathode current not responding to the dynamics of cathode-to-ground voltage, it can still yield accurate reconstructions of future signal values due to the strong presence of the cathode current dynamics in the cathode-to-ground voltage. Finally, in Figure 6(c), the crossmapping of the last set of signals, discharge voltage and cathode-to-ground voltage, indicates two indirect variables that are driven by strong generalized synchrony, with discharge voltage reconstructing cathode-to-ground voltage quite well with a positive time shift of 6 µs. This is likely due to the presence of the strong dynamic driver causing both discharge and cathode-to-ground voltage to respond, but with discharge voltage responding with a shorter



response delay. At the same time, reconstruction in the other direction is significantly lower in cross-mapping skill. This suggests that there may be dynamics present, beyond the common driver dynamics, in the discharge voltage that limits the ability of the cathode-to-ground voltage to capture the behavior accurately.

B. H9 - 4.5kW x2 and x3 Pressure

To elevate the background pressure to two and three times that of the baseline pressure, krypton was released from a ½" Swagelok elbow located 1.8 m downstream of the thruster face and oriented down towards the floor of the chamber. The thruster was allowed to equilibrate for at least two hours at each elevated pressure. The extended cross-convergent mapping results of the voltage and current signals collected while operating at these two pressures are shown in Figure 7 and Figure 8. In most cases, the peak value of the cross-mapping of the signals decreased with pressure. However, not all reconstructions of a pair of signals were affected evenly, with outsized impacts on cathode-to-ground voltage cross-mappings.

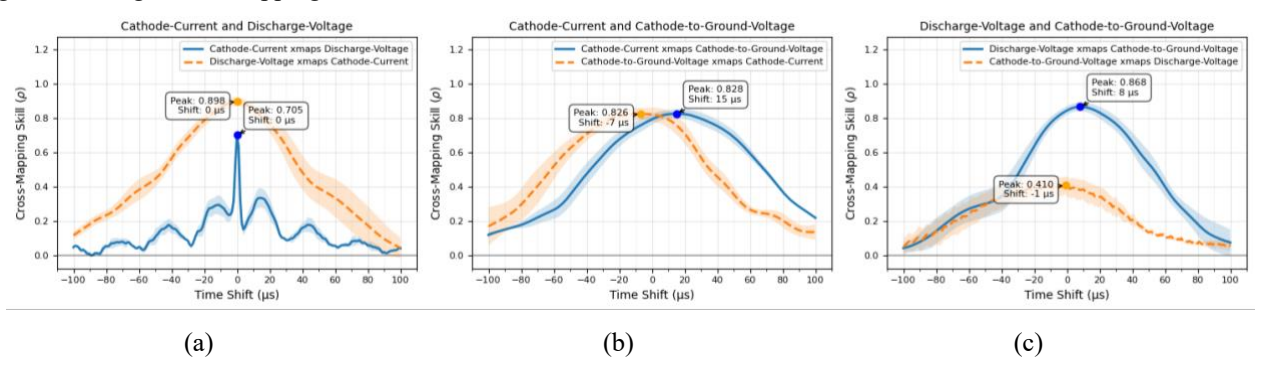


Figure 7: Cross-mapping skill of Hall thruster telemetry of the H9 thruster operating at 300V 15A at 1.5×10⁻⁵ Torr.

With the H9 operating two times the baseline pressure, Figure 7(a) shows the peak of discharge voltage cross-mapping cathode current is now peaked at no time shift. This is likely due to a subtle shift in the response that may be below the analysis time step resolution, and does not necessarily preclude the same causal relations described for Figure 6(a). The cathode-to-ground voltage cross-mapping the cathode current in Figure 7(b) was reduced to below the peak of the cathode current cross-mapping the cathode-to-ground voltage. This reduces the strength of the observed causal relationship of discharge voltage with cathode current and may even indicate that the cathode-to-ground voltage is indirectly affected by cathode current. No significant changes are seen in the cross-mapping of cathode to ground voltage and discharge voltage in Figure 7(c), although a lowering of cross-mapping skill indicates less mutual dynamic information is present in the time series of the two signals.

With the H9 thruster operating at three times the baseline pressure, the trends in cross-mapping skill continue with declining cross-mapping skill in almost all signals. Figure 8(a) indicates that the discharge voltage relationship with cathode current is roughly similar, with a slight lowering in the peak cross-mapping skills. The trend of reduced cross-mapping skill continues to impact cathode-to-ground voltage used to cross-map cathode current (Figure 8(b)), resulting in a peak cross-mapping skill that reconstructs cathode current below generalized synchrony that drives the reconstruction of the cathode-to-ground voltage by cathode current. This indicates that more dynamic information about cathode current is being lost in the history of the cathode-to-ground voltage time series. Finally, cross-mapping of the discharge voltage and cathode current, Figure 8(c), shows a similar trend of decreasing cathode-to-ground cross-mapping skill, while the general synchrony can still accurately reconstruct the cathode current with a positive shift of 7µs. The loss in ability to reconstruct the discharge voltage can be due to an increase in complexity of discharge voltage, or, more likely, given reductions in cathode-to-ground cross-mapping cathode current, the cathode-to-ground voltage is losing mutual dynamic information with the other signals.



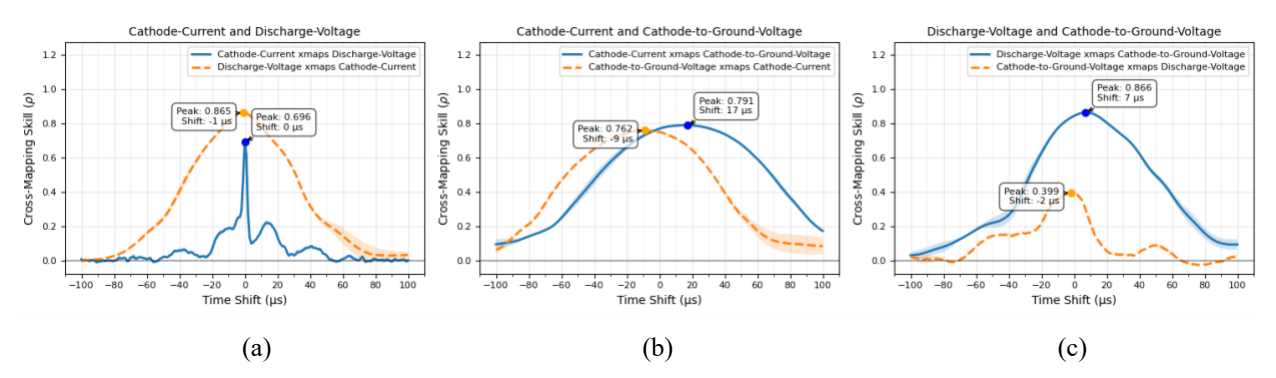


Figure 8: Cross-mapping skill of Hall thruster telemetry of the H9 thruster operating at 300V 15A at 2.1×10⁻⁵ Torr.

IV.Discussion

The necessity to operate Hall thrusters with a single power supply circuit allows a unique opportunity to use simple current and voltage probes throughout the circuit to understand how these signals change in time. The nature of the dynamics in the system travels throughout the circuit and may be observed for dynamic analysis. The easiest of which to access, and are commonly done so in thruster testing, are discharge voltage (measured between the anode and cathode leads near the thruster), discharge current (usually measured with a current clamp on the cathode or anode lead), as well as cathode-to-ground voltage (usually evaluated as a proxy for cathode coupling voltage). In the framework of extended cross-convergent mapping, we are concerned with how the dynamics of each signal interact with one another and use them to identify causal relationships in the system. As demonstrated here and in previous work with Hall thruster signals [6], systems with strong generalized synchrony can still make interpretation of results difficult. In addition, if an incomplete number of the dynamic variables that are used for identifying causal trends, then mapping of causal networks can be difficult. However, there are still two areas under which this causal analysis of an incomplete number of system parameters is useful.

The first is in the identification of relevant dynamic probes to include in simulations of dynamic systems. For example, if dynamic simulations include features, in our case circuit elements, that are not expected to exhibit causally related dynamics to the physics of interest, model validation against these features may not be useful. Previous work has indicated that inclusion of the circuit used to operate the plasma device is key in capturing observed hysteresis behavior of the plasma system [13]. However, if modeling the circuit element of the device that has no causal dynamic relation to the signal of interest, then its inclusion will not add significant dynamic information to the model. In the results presented here, we indicate that discharge voltage often has one of the highest reconstruction skills when used to cross-map the cathode current and cathode-to-ground voltages. Although the direct causal relationship of the discharge voltage to the other two telemetry signals may be quantitatively ambiguous, its ability to reconstruct the other signals with the highest Pearson coefficient between the reconstructed and test signals indicates it is likely responding to many of the same dynamics, although possibly indirectly, and its inclusion in the modeling of the system would be dynamically useful.

The other utility in this analysis is a broader understanding of how dynamic relationships are affected by some parametric evaluation, for example, chamber pressure. Although the direction and degree of a causal relationship between cathode-to-ground voltage and anode voltage may be ambiguous and influenced to a large degree by the general synchronicity of the signals, it is clear to see that these relationships are degraded with increasing pressure. Figure 9 shows how the peak cross-mapping skill of each signal decreased with increasing pressure; however, some relationships are more strongly affected than others. Cathode-to-ground voltage responded more significantly to increasing pressures than the other two telemetry signals, with the causal relationship with cathode current affected by about a 15% reduction in cross-mapping skill. The relationship between cathode-to-ground voltage and discharge voltage experienced a roughly 18% decline in reconstruction quality, with the majority of the decrease occurring at two times baseline pressure. Whether this is due to changes in causality or loss of synchronicity, the result is still



progressive loss of mutual dynamic information needed for reconstruction. Closer examination of the circuit containing the time-varying signals provides insight into where this loss can be occurring. In this case, the loss is observed between the cathode-to-ground and the other parts of the system, the discharge voltage, and the cathode current. This would mean that the information in the time-varying discharge voltage or cathode current is lost in the dynamic history of cathode-to-ground voltage, such that near neighbors selected in the cathode-to-ground voltage training data are well mapped to the discharge voltage or cathode-to-ground voltage manifolds. This could arise as improved pathways between the cathode and ground electrodes improve. This would result in a change in the dynamic information in the cathode-to-ground voltage signal as charge exchange plasmas, more prevalent at higher pressures, affect the cathode potential relative to ground.

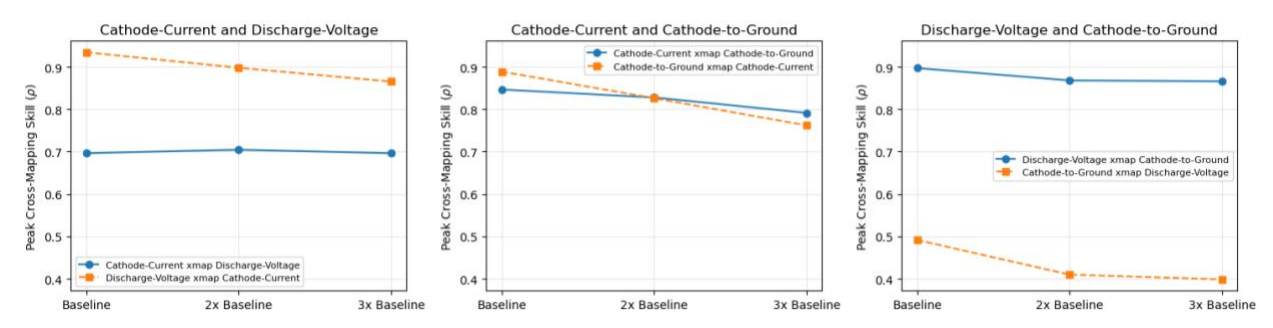


Figure 9: The peak cross-mapping skill of each pair of signals at the three pressure conditions.

V.Conclusion

We applied a dynamic causality analysis technique, extended cross-convergent mapping, to commonly measured thruster telemetry measurements of cathode current, discharge voltage, and cathode-to-ground voltage collected from an H9 Hall thruster operated at 300V and 15A at three background pressures. Parametric sweeps of embedding parameters were used to identify preferred time delay (τ) and embedding dimension (m) for reconstructions with no time shifts. These embedding values were then used for all time shifts for the unique mapping of one signal to the other. Initial evaluation of the cross-mapping skill and the respective peak shifts indicated that discharge voltage is causally influenced by cathode current but with a short time delay, and cathode-to-ground voltage appeared to be unidirectionally influenced by cathode current. Subsequent evaluation of cathode-to-ground voltage and cathode current at increasingly higher pressure indicates this relationship may be driven by generalized synchrony at the higher pressures due to the reduction in cross-mapping skill of cathode-to-ground voltage, which may indicate indirect causal relationships. Although discharge voltage can reconstruct the cathode-to-ground voltage well, the positive time shift peak in cross-mapping skill indicates it is likely due to generalized synchrony. In contrast, cathode-to-ground voltage appears to be weakly responsive to discharge voltage, indicating an indirect relationship as demonstrated in the example problem data set. Apart from the cathode current cross-mapping discharge voltage, which appeared to retain the same degree of synchrony across all pressures, all other cross-mappings were reduced with increasing chamber pressure.

We discuss how, even with a limited subset of system variables monitored, extended cross-convergent mapping of time-varying telemetry signals can still prove useful. One application of the technique is the identification of dynamically relevant probes to include in time-resolved models. Modeling probes or, in our case, circuit elements that capture many of the system's dynamics are more relevant than those not proven to be relevant to the dynamics of interest. To this end, although discharge voltage does not have a clear causality link in cases where there are strong effects of generalized synchrony, it still retained one of the highest cross-mapping skills across the signals that were analyzed, indicating it would be useful to include in dynamic models of the system and circuit. In addition to dynamic probe selection, the technique can provide a framework for evaluating parametric changes to the system environmental parameters, in our case, pressure. Although causality links were not conclusive for cathode-to-ground voltage, the trend with pressure is indicative of a change pathway for information flow with pressure. Improved current pathways to ground through improved charge exchange were proposed as a potential reason for this.



Next steps in this work will focus on evaluating the analysis process and measurements of interest to evaluate the utility of the information gained. Understanding how choices made in the application of the technique affect observed cross-mapping results will speak to the repeatability and robustness of the observed trends, such as choices made to select embedding parameters, data length, and number of windows. Next, we would like to understand what other commonly collected and available signals may help to clarify the relationships better. For example, anode current was not measured, but many of the results may have indicated periods of time when cathode-to-ground voltage began to lose discharge information. Additionally, evaluating the reproducibility of these results day-to-day and across facilities would reveal which signals are most severely impacted and which relationships remain relatively robust.

Acknowledgments

This work was supported by the NASA Space Technology Research Institute JANUS, Grant Number 80NSSC21K1118.

References

- [1] H. Ye, E. R. Deyle, L. J. Gilarranz, and G. Sugihara, "Distinguishing time-delayed causal interactions using convergent cross mapping," *Sci Rep*, vol. 5, no. 1, p. 14750, 2015, doi: 10.1038/srep14750.
- [2] G. Sugihara *et al.*, "Detecting Causality in Complex Ecosystems," *Science (1979)*, vol. 338, no. 6106, pp. 496–500, Oct. 2012, doi: 10.1126/science.1227079.
- [3] C. E. Huerta, R. S. Martin, D. Q. Eckhardt, and J. W. Koo, "Determining causality in Hall effect thrusters using extended convergent cross mapping, part I**," *Plasma Sources Sci Technol*, vol. 30, no. 7, p. 075004, 2021, doi: 10.1088/1361-6595/ac0a95.
- [4] C. E. Huerta, R. S. Martin, D. Q. Eckhardt, and J. W. Koo, "Determining causality in Hall effect thrusters using extended convergent cross mapping: II*," *Plasma Sources Sci Technol*, vol. 31, no. 3, p. 035015, 2022, doi: 10.1088/1361-6595/ac511e.
- [5] F. Takens, "Detecting strange attractors in turbulence," in *Dynamical Systems and Turbulence, Warwick 1980*, D. Rand and L.-S. Young, Eds., Berlin, Heidelberg: Springer Berlin Heidelberg, 1981, pp. 366–381.
- [6] C. Huerta, C. Greve, and A. Wong, "Comparison of causality determination techniques in studying Hall-effect thrusters," *Journal of Electric Propulsion*, vol. 3, no. 1, p. 23, 2024, doi: 10.1007/s44205-024-00084-z.
- [7] C. M. Greve, K. Hara, R. S. Martin, D. Q. Eckhardt, and J. W. Koo, "A data-driven approach to model calibration for nonlinear dynamical systems," *J Appl Phys*, vol. 125, no. 24, p. 244901, Jun. 2019, doi: 10.1063/1.5085780.
- [8] H. Kantz and T. Schreiber, *Nonlinear time series analysis*. Cambridge University Press, 2003.
- [9] R. S. Martin, C. M. Greve, C. E. Huerta, A. S. Wong, J. W. Koo, and D. Q. Eckhardt, "A robust time-delay selection criterion applied to convergent cross mapping," *Chaos: An Interdisciplinary Journal of Nonlinear Science*, vol. 34, no. 9, p. 093110, Sep. 2024, doi: 10.1063/5.0209028.
- [10] J. Cabrera, D. Jovel, and M. L. R. Walker, "Pressure Facility Effects on the Impedance Characteristics of a 9-kW HET," in *38th International Electric Propulsion Conference*, Toulouse, France, 2024.
- [11] R. R. Hofer, S. E. Cusson, R. B. Lobbia, and A. D. Gallimore, "The H9 magnetically shielded Hall thruster," in *35th International Electric Propulsion Conference*, Electric Rocket Propulsion Society, 2017, pp. 2017–2232.
- [12] C. M. Greve and C. Marsh, "Evaluating Hall thruster startup transients using dynamics-based embeddings," *Journal of Electric Propulsion*, vol. 4, no. 1, p. 36, 2025, doi: 10.1007/s44205-025-00136-y.
- [13] Y. Yamashita, K. Hara, and S. Sriraman, "Hysteresis between gas breakdown and plasma discharge," *Phys Plasmas*, vol. 31, no. 7, p. 073510, Jul. 2024, doi: 10.1063/5.0198151.

